



# Effects of heavy alkali elements in Cu(In,Ga)Se<sub>2</sub> solar cells with efficiencies up to 22.6%

Philip Jackson\*, Roland Wuerz, Dimitrios Hariskos, Erwin Lotter, Wolfram Witte, and Michael Powalla


Zentrum für Sonnenenergie- und Wasserstoff-Forschung Baden-Württemberg (ZSW), Industriestraße 6, 70565 Stuttgart, Germany

Received 28 June 2016, revised 6 July 2016, accepted 6 July 2016

Published online 12 July 2016

**Keywords** CIGS, thin-film solar cells, high efficiency, alkali elements

\* Corresponding author: e-mail philip.jackson@zsw-bw.de, Phone: +49 711 7870 260, Fax: +49 711 7870 230

 This is an open access article under the terms of the Creative Commons Attribution-NonCommercial-NoDerivs License, which permits use and distribution in any medium, provided the original work is properly cited, the use is non-commercial and no modifications or adaptations are made.

We report on the use and effect of the alkali elements rubidium and caesium in the place of sodium and potassium in the alkali post deposition treatment (PDT) as applied to Cu(In,Ga)Se<sub>2</sub> (CIGS) solar cell absorbers. In order to study the effects of the different alkali elements, we have produced a large number of CIGS solar cells with high efficiencies resulting in a good experimental resolution to detect even small differences in performance. We examine the electrical device

parameters of these fully functional devices and observe a positive trend in the  $I$ - $V$  parameters when moving from devices without PDT to KF-, RbF-, and eventually to CsF-PDT. A diode analysis reveals an improved diode quality for cells treated with heavier alkalis. Furthermore, secondary ion mass spectrometry (SIMS) measurements reveal a competitive mechanism induced within the class of alkali elements in the CIGS absorber induced by the alkali post deposition treatment.

**1 Introduction** Since the introduction of the alkali element sodium Na in the 1990's [1] into the research of Cu(In,Ga)Se<sub>2</sub> (CIGS) type solar cells, the investigation of the role of alkali elements in such photovoltaic materials has spawned a large number of studies and publications on that topic over the following decades, e.g. [2–5]. From early experiments with other alkali elements by using alkali fluoride precursors for doping of CIGS layers, it was concluded that Na is the most effective alkali element for increasing the efficiency of CIGS solar cells [6]. Despite these findings and despite the long and intensive study of the effect of Na on CIGS solar cells, another major step in CIGS research could be taken within this very same field of investigation just recently. By discovering the beneficial effects of a different alkali element for CIGS (i.e. potassium) and by the deliberate use thereof by post deposition treatment (PDT), device performance could be boosted once more [7–9]. Again a whole new realm of scientific investigations was opened leading to a fast rise of record efficiencies by using this technique: 20.4% to 21.0% (EMPA: 20.4% [9], ZSW: 20.8% [10], Solibro 21.0% [11]). In this contribution we show how we have followed this logic even further by introducing two

more alkali elements. We describe the impact such new elements have on CIGS device performance and also some interactions between alkali elements in the absorber material.

## 2 Experimental methods

**2.1 Processing of CIGS cells** In our standard procedure for high-efficiency CIGS solar cell manufacturing, we begin with washing the alkali-aluminosilicate glass substrate. Next, we deposit a thin film of sputtered molybdenum (500–900 nm). Then we co-evaporate Cu, In, Ga, and Se to grow the CIGS semiconductor layer in a multi-stage process (2.5–3.0 μm). After the CIGS process, we perform an alkali post deposition treatment PDT similar to the procedure employed in Ref. [9]. After taking these samples out of the vacuum chamber, we dip these into a chemical bath to form a thin layer of CdS (30–50 nm). On top of that, we sputter (Zn,Mg)O or undoped ZnO (50–100 nm), and Al-doped ZnO (150–200 nm). Finally, we evaporate a nickel/aluminium/nickel grid for contacting the completed cell. The resulting cell area is about 0.5 cm<sup>2</sup>. For high-efficiency cells we also evaporate an anti-reflective coating (ARC) of MgF<sub>2</sub> on top of the whole cell stack.

**2.2 Characterisation** For the analytical description of the CIGS solar cells, current–voltage ( $I$ – $V$ ) analysis was performed under a simulated AM 1.5 G spectrum at 25 °C with a four-point measurement setup. The obtained data was further analysed by diode analysis according to the one-diode model. In addition, we have measured the integral CIGS composition with an X-ray fluorescence spectroscopy (XRF) instrument from EDAX (Eagle XXL). The determined compositional ratio values as the Cu/(Ga + In) (CGI) and Ga/(Ga + In) (GGI) ratios represent average values that do not further specify the compositional grading in the depth of the CIGS absorber as shown in [12]. In order to determine the amount of the various alkali elements in the CIGS absorber, secondary ion mass spectrometry (SIMS) was performed in a LEYBOLD LHS 10 system with a secondary ion and neutral mass spectrometer module (SSM 200) using a Balzers 511 quadrupole for mass separation. For actual quantification we have produced implantation standards and have again measured these with SIMS to obtain a calibration curve for various alkali elements in device related CIGS material.

**3 Results and discussion** The deliberate introduction of potassium by PDT to CIGS and its large impact in the form of a significant  $V_{oc}$ -gain in devices and also its potential to give a better access to high band gap CIGS devices [10], has led us to the assumption that the heavier alkali elements rubidium Rb and caesium Cs could evidence even more beneficial effects for device manufacturing if applied with the PDT method.

In order to compare the effect of the different alkali elements applied by PDT in a statistically most relevant way, we have selected a large set of CIGS production runs, that was realised over a two year period between March 2013 and March 2015, including a total number of 1491 CIGS solar cells. All these cells were produced without an ARC. Although some differences remain between these runs over this long time period, we have applied as many selection criteria as possible to ensure the highest degree of comparability as possible. For example, only CIGS solar cells with the same chemical bath deposited (CBD) buffer, CdS, were included and also the range of possible CIGS absorber compositions of the individual solar cells was restricted to the following ranges:  $0.88 \leq CGI \leq 0.92$  and  $0.30 \leq GGI \leq 0.33$ . Also only efficiencies greater or equal to 15.0% (w/o ARC) were included in order to avoid irrelevant data that is often due to trivial reasons without any significance with regards to device physics.

Figure 1 displays the result of this comparison by way of comparing boxplots and median values of solar cell efficiency (ETA) without ARC, open-circuit voltage ( $V_{oc}$ ), fill-factor (FF), and short-circuit current density ( $J_{sc}$ ) with various alkali compounds (potassium fluoride KF, rubidium fluoride RbF, and caesium fluoride CsF) used for PDT as a variable.

It has to be noted that most data sets for each individual alkali compound used for PDT are skewed for each re-

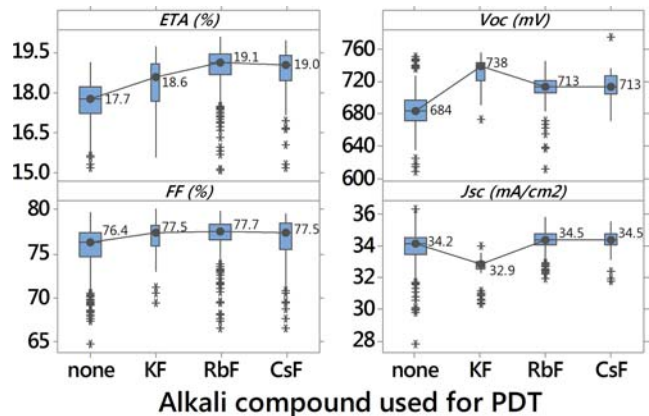


**Figure 1** Boxplot of solar cell efficiency (ETA) without ARC, open-circuit voltage ( $V_{oc}$ ), fill-factor (FF), and short-circuit current density ( $J_{sc}$ ) with various alkali compounds (KF, RbF, CsF) used for PDT. There is a beneficial trend in median efficiency values towards heavier alkalis in PDT application.

spective  $I$ – $V$  parameter. This, however, is a quite common appearance. For that reason more outlier values (marked with asterisks) are present than one would generally expect for normally distributed data. The comparison of the median values still shows a very clear trend towards higher efficiencies when moving from no PDT to heavier alkali-

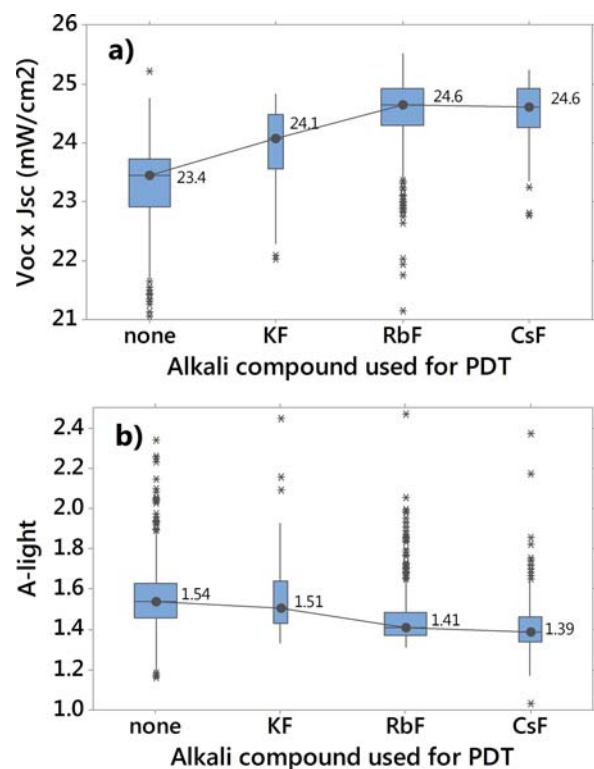


**Figure 2** Further analysis of  $I$ – $V$  data. (a) The consistent trend in efficiency when moving up to heavier alkali elements for PDT is constituted by the trend in  $V_{oc} \times J_{sc}$ . (b) A diode analysis reveals a similar trend in this direction by the reduction of the ideality factor  $A$ -light (derived from the illuminated  $I$ – $V$  curve).

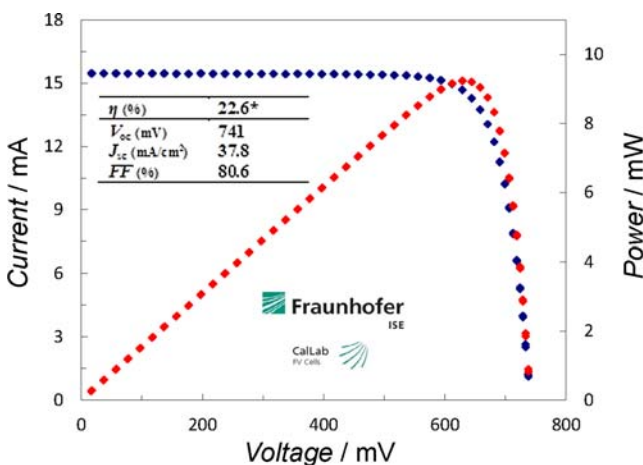
**Table 1** List of former and current ZSW record results and the PDT-methods applied.

PDT	$\eta$ (%)	$V_{oc}$ (mV)	$J_{sc}$ (mA/cm <sup>2</sup> )	FF (%)	date of publication
N/A	20.3*	740	35.4	77.5	01/2011 [13]
KF	20.8*	757	34.8	79.1	02/2014 [10]
RbF	21.7*	746	36.6	79.3	12/2014 [14]
RbF	22.0*	744	36.7	80.5	03/2016 [15]
RbF	22.6*	741	37.8	80.6	this work

\* Independently certified by Fraunhofer ISE.

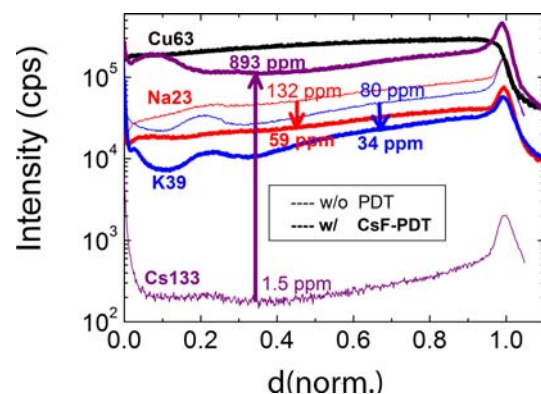
compounds used for PDT. In particular, one can see that there is, in fact, an additional benefit from going beyond potassium to rubidium and caesium.

This gain in efficiency for all alkali compounds is due to a gain in  $V_{oc}$ . However, the trend in  $V_{oc}$  is not as consistent as in ETA since the gain in  $V_{oc}$  for KF-PDT is higher than for RbF- or CsF-PDT. Yet, CIGS solar cells with RbF- and CsF-PDT still exhibit higher efficiencies due to the accompanying loss in  $J_{sc}$  for KF-PDT. The cause for the consistent trend in efficiency can be seen when we multiply the factors  $V_{oc}$  and  $J_{sc}$  as depicted in Fig. 2(a). There we see that the gain in  $V_{oc}$  for KF-PDT is larger than the loss in  $J_{sc}$  and that the overall gain of  $V_{oc}$  combined with the respective  $J_{sc}$  values is even higher for RbF-PDT and CsF-PDT. One explanation for this positive trend in  $V_{oc}$  and device performance towards heavier alkali elements in PDT, is the improvement of diode quality as expressed by the ideality  $A$ -light (derived from the illuminated  $I$ - $V$  curve by diode analysis with a one-diode model) (see Fig. 2(b)). A similar trend can be seen in the saturation current density (not shown here). Apart from that, we also find in the bottom left plot of Fig. 1 a very slight positive gain in FF for the alkali treated CIGS cells. In addition to average or median values we also see a positive efficiency trend towards heavier alkalis applied with PDT in the ZSW record de-


**Figure 3**  $I$ - $V$  curve of the most current PDT-treated CIGS solar cell with an efficiency of 22.6%\* (\*certified by Fraunhofer ISE).

vices as listed in Table 1. With this we demonstrate that the above results, obtained with the large data set, have a high degree of relevance even for high efficiency CIGS devices. The  $I$ - $V$  curve of the most current device is displayed in Fig. 3.

In order to better understand the mechanisms involved in the PDT procedure with these different alkali elements, we have performed a depth profiling analysis with secondary ion mass spectrometry (SIMS). However, before being able to actually quantify the alkali elements with this method, we had to produce and measure implantation standards for each element. By that we are able to compare the absolute alkali content in PDT cells and in those without PDT. The resulting general observation is that the heavier alkalis, that are introduced by PDT into the already grown CIGS absorber, tend to push out the lighter alkalis already present in the material (Na and K). This applies for all alkali compound PDT's described in this contribution (KF, RbF, and CsF). By way of example, we have plotted such a depth profile comparison for two samples with (thick lines) and without CsF-PDT (thin lines) in Fig. 4. Both samples originate from the same CIGS run from positions in the CIGS deposition field directly beside each other so as to guarantee true comparability apart from PDT. Thus it is now possible to compare the sodium and potassium levels in both samples and correlate the difference with PDT. The copper signal is taken as a reference level for both SIMS measurements to determine the alkali concentrations. Both signals lie more or less on top of each other. This fact ensures that a comparison of the absolute levels of the alkali signals is legitimate. In addition, the copper signal also indicates the range in which the CIGS compound is present. For the sake of clarity in graph of Fig. 4 all other elements have been omitted. With that we can now clearly see that by CsF-PDT the absolute content of sodium and potassium


**Figure 4** SIMS depth profile of CIGS absorber without (thin lines) and with CsF-PDT (thick lines) (CIGS surface is located at the normalised depth  $d$  (norm.) = 0). By comparing the two sets of alkali profiles of the alkali isotopes Na23, K39, and Cs133, it becomes apparent that the heavier alkali Cs pushes out the lighter alkalis in PDT. The same was observed for Rb (not shown here). Both Cu63 lines lie on top of each other thus ensuring comparability of the alkali signals of the two samples.



is reduced from 132 ppm to 59 ppm and from 80 ppm to 34 ppm respectively. This reduction, however, is not only observed at the surface of the CIGS absorber from where the PDT is applied, but is effectuated throughout the whole depth of the absorber.

Atom probe tomography (APT) analysis on CIGS devices showed accumulation of sodium at grain boundaries, but nevertheless concentration of sodium in the bulk is comparable to the integral concentration of Na in the grain boundaries [16, 17]. Later a similar finding was also published for potassium [18]. So far it is unclear whether Rb and Cs push away Na and K only along the grain boundaries or also in the bulk of the grains. APT measurements of CIGS layers after PDT with Rb will hopefully give an answer to this question in the near future.

**4 Conclusion** We have further developed the alkali post deposition treatment (PDT) for CIGS solar cells by successfully introducing the heavier alkali elements rubidium and caesium. Significant performance gains could be demonstrated for CIGS devices treated with RbF- or CsF-PDT compared to KF-PDT or no-PDT devices. The reason for that appears to be a better diode quality. Furthermore, a SIMS analysis has provided insight into some of the competitive mechanisms that take place within the CIGS absorber induced by PDT with heavier alkali elements: The lighter alkali elements are being driven out of the absorber. Future studies will have to more directly prove whether this process predominantly takes place at the grain boundaries or not.

**Acknowledgements** We gratefully acknowledge the support of the ZSW MAT team – in particular that of Dieter Richter – for their technical management of the small area production line and their efforts in the actual production of the solar cells. We also thank A. Eicke for SIMS measurements and thankfully acknowledge the funding by the German Federal Ministry of Economics and Technology (BMWi) under contract- no. 0325715. This work has also received funding from the European Union's Horizon 2020 research and innovation programme under grant agreement no. 641004.

## References

- [1] J. Hedstrom, H. Ohlsen, M. Bodegard, A. Kylner, L. Stolt, D. Hariskos, M. Ruckh, and H. W. Schock, ZnO/CdS/Cu(In,Ga)Se<sub>2</sub> thin film solar cells with improved performance, in: Conference record of the 23rd IEEE Photovoltaic Specialists Conference, pp. 364–371 (1993).
- [2] T. Nakada, D. Iga, H. Ohbo, and A. Kunioka, Jpn. J. Appl. Phys. **36**, 732 (1997).
- [3] D. Braunger, D. Hariskos, G. Bilger, U. Rau, and H.-W. Schock, Thin Solid Films **361**, 161–166 (2000).
- [4] D. Rudmann, Effects of sodium on growth and properties of Cu(In, Ga)Se<sub>2</sub> thin films and solar cells, Doctoral dissertation, Eidgenössische Technische Hochschule ETH Zürich, No. 15576, 2004.
- [5] P. T. Erslev, J. W. Lee, W. N. Shafarman, and J. D. Cohen, Thin Solid Films **517**, 2277–2281 (2009).
- [6] M. A. Contreras, B. Egaas, P. Dippo, J. Webb, J. Granata, K. Ramanathan, S. Asher, A. Swartzlander, and R. Noufi, Conference record of the 26th IEEE Photovoltaic Specialists Conference, 30 September–3 October 1997, Anaheim, California, pp. 359–362.
- [7] D. Rudmann, A. F. da Cunha, M. Kaelin, F. Kurdesau, H. Zogg, A. N. Tiwari, and G. Bilger, Appl. Phys. Lett. **84**, 1129 (2004), DOI: 10.1063/1.1646758.
- [8] A. Laemmle, R. Wuerz, and M. Powalla, Phys. Status Solidi RRL **7**, 631 (2013), DOI: 10.1002/pssr.201307238.
- [9] A. Chirilă, P. Reinhard, F. Pianezzi, P. Bloesch, A. R. Uhl, C. Fella, L. Kranz, D. Keller, C. Gretener, H. Hagedorfer, D. Jaeger, R. Erni, S. Nishiwaki, S. Buecheler, and A. N. Tiwari, Nature Mater. **12**, 1107 (2013), DOI: 10.1038/nmat3789.
- [10] P. Jackson, D. Hariskos, R. Wuerz, W. Wischmann, and M. Powalla, Phys. Status Solidi RRL **8**, 219 (2014), DOI: 10.1002/pssr.201409040.
- [11] D. Herrmann et. al., CIGS module manufacturing with high deposition rates and efficiencies, presented at 40th IEEE PVSC, Denver, CO, USA, June 8–13, 2014.
- [12] M. Powalla, P. Jackson, W. Witte, D. Hariskos, S. Paetel, C. Tschamber, and W. Wischmann, Sol. Energy Mater. Sol. Cells **119**, 51 (2013), DOI: 10.1016/j.solmat.2013.05.002.
- [13] P. Jackson, D. Hariskos, E. Lotter, S. Paetel, R. Wuerz, R. Menner, W. Wischmann, and M. Powalla, Prog. Photovolt.: Res. Appl. **19**, 894 (2011), DOI: 10.1002/pip.1078.
- [14] P. Jackson, D. Hariskos, R. Wuerz, O. Kiowski, A. Bauer, T. M. Friedlmeier, and M. Powalla, Phys. Status Solidi RRL, **9**, 28–31 (2015), DOI: 10.1002/pssr.201409520.
- [15] Press release: ZSW Sets European Record of 22 Percent for CIGS Cells, Stuttgart, March 31, 2016, [https://www.zsw-bw.de/fileadmin/user\\_upload/PDFs/Pressemitteilungen/2016/pi07-2016-ZSW-CIGS22Percent-en.pdf](https://www.zsw-bw.de/fileadmin/user_upload/PDFs/Pressemitteilungen/2016/pi07-2016-ZSW-CIGS22Percent-en.pdf).
- [16] E. Cadel, N. Barreau, J. Kessler, and P. Pareige, Acta Mater. **58**, 2634–2637 (2010).
- [17] R. Schlesiger, C. Oberdorfer, R. Wuerz, G. Greiwe, P. Stender, M. Artmeier, P. Pelka, F. Spaleck, and G. Schmitz, Rev. Sci. Instrum. **81**, 043703 (2010).
- [18] O. Cojocaru-Miredin, P.-P. Choi, D. Abou-Ras, S. S. Schmidt, R. Caballero, and D. Raabe, IEEE J. Photovolt. **1**, 207 (2011).